phys. stat. sol. (c) **2**, No. 2, 795–800 (2005) / **DOI** 10.1002/pssc.200460303

Waveguide-plasmon polaritons in photonic crystal slabs with metal nanowires

S. G. Tikhodeev[*, 1], **N. A. Gippius**[1], **A. Christ**[2], **T. Zentgraf**[2], **J. Kuhl**[2], and **H. Giessen**[3]

[1] A. M. Prokhorov General Physics Institute RAS, Vavilova 38, Moscow 119991, Russia
[2] Max-Planck-Institut für Festkörperforschung, 70569 Stuttgart, Germany
[3] Institute of Applied Physics, University of Bonn, 53115 Bonn, Germany

Received 16 July 2004, revised 31 August 2004, accepted 14 January 2005
Published online 15 February 2005

PACS 42.70.Qs, 42.79.Gn, 71.36.+c, 73.20.Mf, 78.66.–w

The optical properties of a photonic crystal slab made of periodic arrays of gold nanowires on top of different dielectric substrates, supporting and not supporting the guided modes are discussed. While only Rayleigh-type anomalies are observed for thin dielectric substrates, thicker waveguiding substrates demonstrate strong coupling phenomena. It is shown that the interaction between the quasiguided modes in the photonic crystal slab and the localised plasmons in metal nanostructures results in the formation of a strongly coupled waveguide-plasmon polariton. The formation of the new quasiparticle manifests itself in the strong anticrossing between quasiguided modes and plasmon resonances in the measured as well as calculated optical spectra. The effect opens new possibilities for photonic band gap engineering in metallic-dielectric photonic crystals.

Photonic crystals (PhC) are materials periodically structured on a sub-micrometer scale. Their properties have been the subject of extensive research activities in recent years starting from the pioneering works by E. Yablonovitch and S. John [1, 2]. A rich variety of important optical phenomena has been demonstrated [3–5]. However, the history of the investigations of the optical properties in spatially periodic structures is actually much longer. In particular, we are celebrating now the centenary of the seminal works [6, 7]: Professor Wood observed the famous Wood's anomalies in the diffraction grating spectrum, and Lord Rayleigh explained one type of them (diffractive or Rayleigh's anomaly) by a passing off of a spectrum of higher order. Diffraction gratings are simple realizations of one-dimensional (1D) spatially periodic planar photonic crystal slabs (PhCS), and different Wood's anomalies are the most prominent effects in the optical spectra of PhCS.

Initially, the PhC structures were mainly built of transparent dielectric materials with different nondispersive refractive indices. However, nowadays considerable effort is devoted to the investigation of *polaritonic* photonic crystal structures with complex unit cells, containing nanostructured semiconducting or metallic materials [8–12]. Such polaritonic crystals are particularly attractive because of their ability to control electronic and photonic resonances simultaneously. Therefore, such structures may open up further impressive possibilities for tailoring the light-matter interaction.

Various photonic crystal structures with nanostructured metals have been realized so far. In addition to periodically modulated metal surfaces, including surface corrugation [13–16] and hole arrays [17] especially regular arrangements of individual metal nanoparticles on dielectric substrates [18] are prominent examples of such polaritonic crystal structures. Large photonic band gaps [19], extraordinary light trans-

[*] Corresponding author: e-mail: tikh@gpi.ru, Phone: +7 095 132 81 02, Fax: +7 095 234 31 96

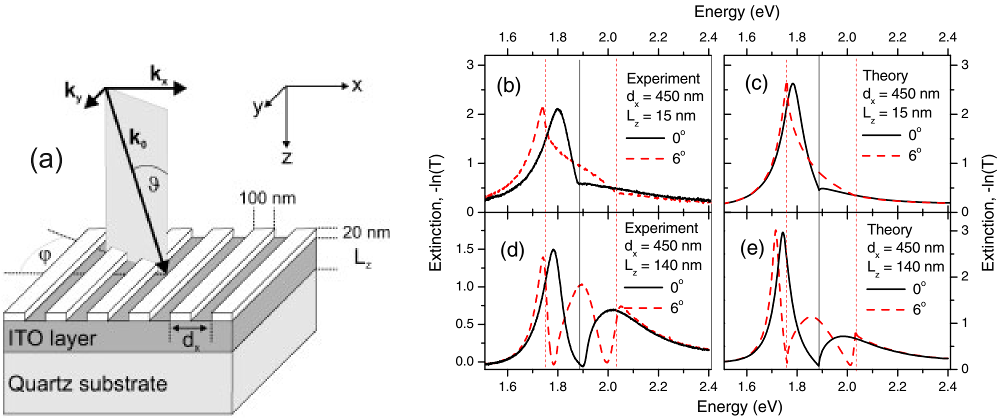

Fig. 1 Schematics of the metal-dielectric structure (a). Measured (b, d) and calculated (c, e) extinction spectra ($-\ln T$, T – transmissivity) in p-polarisation ($\varphi = 0$, electric field perpendicular to the wires) of the metal-dielectric structures with thin (15 nm: b, c) and thick (140 nm: d, e) ITO layer [21, 22]. Period of the structures is $d_x = 450$ nm. The energies of $g = 1$ Rayleigh anomalies Eq. (1) for diffraction into substrate for normal $\vartheta = 0°$ and $\vartheta = 6°$ incidence are shown by vertical solid and dashed lines, respectively.

mission properties through arrays of subwavelength holes [17], negative refraction [20], and strong coupling effects between electronic and photonic resonances [21, 22] have been demonstrated. The particular optical properties of these metallic nanostructures can be attributed to the excitation of so-called particle or surface plasmons [23, 24]. These electronic excitations are a consequence of the collective oscillation of the conduction band electrons in the metal. They manifest themselves in a strong field enhancement near the metal surface. In case of periodic structures, a strong modification of the optical response of these plasmon resonances takes place, because of the far-field interaction between the nanoparticles via the Bragg resonances.

In this paper, we analyse experimentally and theoretically the optical properties of periodic gold nanowire arrays deposited on a dielectric ITO layer on top of a quartz substrate [21, 22]. The structure and the geometry of light incidence is shown schematically in Fig. 1a. The examples of extinction spectra (measured and calculated via the *S*-matrix method [25]) are shown in Figs. 1b–e for a structure with period $d_x = 450$ nm.

If the ITO layer is thin enough that it does not support guided modes in the investigated range of photon energies, the extinction spectra in p-polarisation ($\varphi = 0$, electric field perpendicular to the wires) show a single pronounced peak, due to the excitation of a nanowire plasmon with resonance energy about 1.8 eV. Cusp-like structures seen in Figs. 1b, c are Rayleigh anomalies due to opening of $g = 1$ diffraction channel into the quartz substrate ($\varepsilon = 2.14$). They correspond to photon energies [7]

$$\omega_{\text{Rayleigh}} = \frac{2\pi g c}{\sqrt{\varepsilon}\,(1 \pm \sin\vartheta)\, d_x}, \qquad g = 1, 2, \dots, \tag{1}$$

see thin vertical solid (for $\vartheta = 0$) and dashed (for $\vartheta = 6°$) lines in Figs. 1b–e. With a change of incidence angle ϑ, as well as of the period of the structure d_x (see Ref. [22] for more details), the Rayleigh anomalies are shifted in agreement with Eq. (1).

The extinction spectra are modified drastically if the ITO layer is thick enough to support the guided modes (see Figs. 1d, e). In case of normal incidence and in resonance structures with a period of ~ 450 nm, the single plasmon extinction peak is split into a pair of peaks (solid curves). Under inclined incidence three peaks are clearly visible (dashed curves). The evolution of these peaks with change of period (at normal incidence) and of incidence angle (at periods 450 and 375 nm) are shown in Fig. 2. A strong anticrossing behavior is seen, with huge Rabi splitting of about 250 meV.

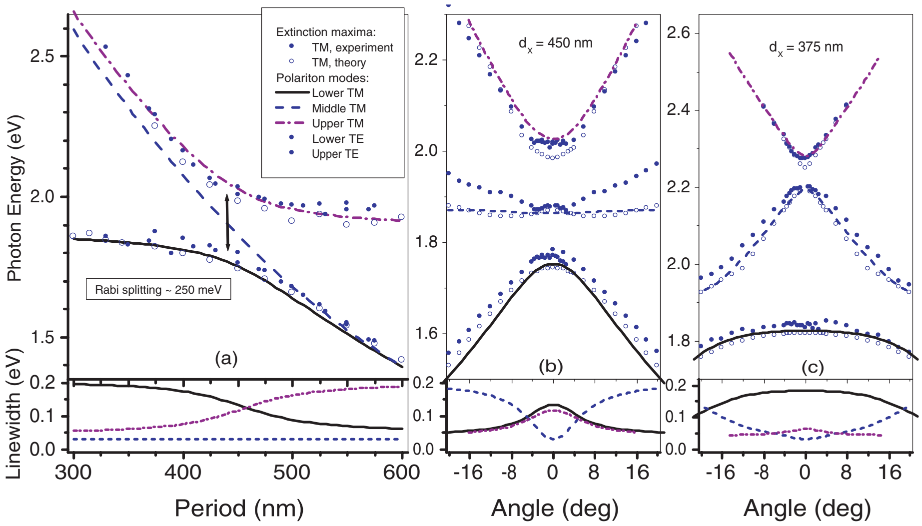

Fig. 2 The calculated (empty circles) and measured (solid circles) energy positions of the extinction maxima in p-polarisation as functions of period for normal incidence (a), and of incidence angle for periods $d_x = 450$ nm (b) and 375 nm (c). Lines show the solutions of the waveguide-plasmon polariton model [21] for real (top panels) and imaginary (bottom panels) parts of the polariton eigenenergies.

The anticrossing behavior in Fig. 2 means the formation of a mixed quasiparticle, a *waveguide-plasmon polariton* [21]. A simple empty lattice type model explained in Fig. 3 allows to understand the behavior of this polariton with change of the period and angle of incidence. (The latter is coupled with the horizontal projection of the photon wavevector via $k = \omega \sin \vartheta / c$). Three polariton branches (lower, middle and upper) appear as a result of a strong coupling between the isolated nanowire plasmon (horizontal dashed line in Fig. 3) and the lowest TM_0 guided mode folded by $k_\pm = \pm 2\pi/d_x$ (dash-dotted lines, intersecting in the center of the 1st Brillouin zone). At normal incidence, $k = 0$, the middle polariton branch in this symmetric structure is antisymmetric and optically inactive. As a result, there exists no middle extinction maximum for the normal incidence.

The real and imaginary parts of the waveguide-plasmon polariton can be easily modelled [21] via the eigenenergies of the effective Hopfield-like Hamiltonian for interacting isolated nanowire plasmon and folded by $k_\pm = \pm 2\pi/d_x$ TM_0 guided model (including the linewidth of these three modes far from the polariton resonance). The resulting dispersions reproduce qualitatively the measured and calculated via S-matrix evolution of the extinction maxima and resonance linewidths, see lines in Fig. 2.

We would like to add that the waveguide-plasmon polariton peaks in the extinction spectra are realizations of Wood's anomalies of another, resonant type. Such anomalies appear when a resonance can interact with photon continuum outside the PhC structure. Resonant Wood's anomalies are also called Fano resonances [26].

All the theoretical results given in Figs. 1, 2 (see also Refs. [21, 22]) and demonstrating a good qualitative agreement with the measured data, are calculated within a scattering matrix method [25] without adjustable parameters. The input parameters of the method are the measured geometrical parameters of the structures and the known dielectric susceptibilities. The dielectric susceptibility of gold was taken from [27], that of ITO was approximated as [28] $\varepsilon_{\mathrm{ITO}}(\lambda) \approx 1 + 1.81302\lambda^2/(\lambda^2 - 0.07597)$ for λ between 0.3 μm and 0.6 μm, and $\varepsilon_{\mathrm{quartz}} = 2.13$.

The scattering matrix method allows also to calculate the near-field distribution in the vicinity of the PhCS. The knowledge of such near-field distributions is not only important for understanding the physical mechanisms of the observed coupling phenomena, but can also help to control the nonlinear optical response in possible future applications. The calculations [22] reveal the existence of a standing wave inside the ITO layer below the gold nanowire gratings. In the case of the resonance, this standing wave has field maxima at the position of the gold nanowires, leading to a large field enhancement near the wires and therefore high extinction values. The extinction minimum between the two polariton branches in contrast is due to a standing wave with anti-nodes between the nanowires and therefore only weak fields at the position of the gold nanowires.

Thus, the *S*-matrix method [29, 30, 25] is a very convenient tool for understanding the optical properties of the metal/dielectric photonic structures. Advantages of the scattering matrix method are: (i) direct calculation of the radiation losses; (ii) easiness to find optically active as well as *inactive* modes; (iii) direct inclusion of any frequency dispersion of the dielectric susceptibilities; (iv) possibility to account for any complex unit cell of photonic crystals; (v) direct connection with the general scattering matrix theory; (vi) exact allowance for the *unitarity* (for transparent materials), *reciprocity*, and *symmetry* properties [31]. Note that the first three (calculation of radiative losses, finding optically inactive modes, and describing frequency dispersive materials) are especially difficult for the numerical algorithms based on the finite difference in time domain (FDTD) method.

Disadvantages of the scattering matrix method are: (i) slow convergence in case of metal/dielectric interfaces; (ii) N^3 CPU time, for a $(N \times N)$-truncated *S*-matrix. We need hundreds of spatial harmonics per dimension for the calculations for metal/dielectric structures. For example, the curves for p-polarization shown in Figs. 1, 2 have been calculated with 301 plane waves, with the estimated relative error about 1%. As a result, the method becomes impractical for 2D periodic metal/dielectric structures. In contrast, already ten harmonics per dimension are sufficient for analogous dielectric structures.

In order to illustrate the power of the *S*-matrix method in calculation of the resonance modes in PhCS, we compare in Fig. 4 the *S*-matrix and FDTD (from [32]) results for the lowest quasiguided modes in a free-standing GaAs slab with a rectangular array of cylindrical holes. A good agreement between both methods is seen. (Note that the FDTD data [32] for $k = 0$ are given only for optically active doublet modes.) However, with the frequency increase the FDTD results for the real parts of eigenenergy (left panel) become increasingly red-shifted against the S-matrix ones. This may be attributed to the finite mesh in FDTD cacluations. Only 37 spatial harmonics were used in the truncated *S*-matrix, and the CPU time needed for the full characterization of each eigenmode in Fig. 4 was only 3 sec (on a personal computer).

In conclusion, we have shown experimentally and theoretically that far-field coupling effects can strongly influence the optical properties of gold nanowire gratings deposited on top of dielectric ITO layers. We demonstrate clearly that the transmission spectra of such photonic crystal structures can change substantially with the substrate thickness. While gold nanowire gratings on top of a thinner ITO layer that does not support optical waveguide modes only induce Wood's diffractive anomalies, structures on top of thicker waveguiding ITO layers can exhibit a much richer behavior. The transmission

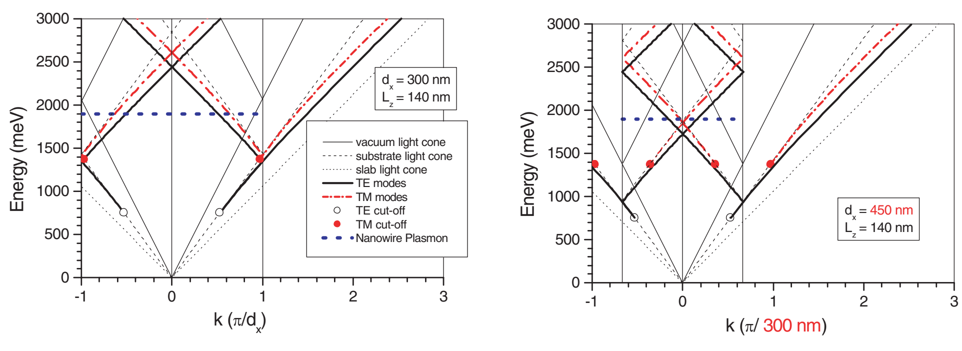

Fig. 3 Schematics of the waveguide-plasmon polariton formation is illustrated in empty lattice approximation. The lowest TE (thick solid lines) and TM (thick dash-dotted) guided modes in the ITO waveguide on a quartz substrate are folded into the 1st Brillouin zone of the structure with periods $d_x = 300$ nm (left panel) and 450 nm (right panel).

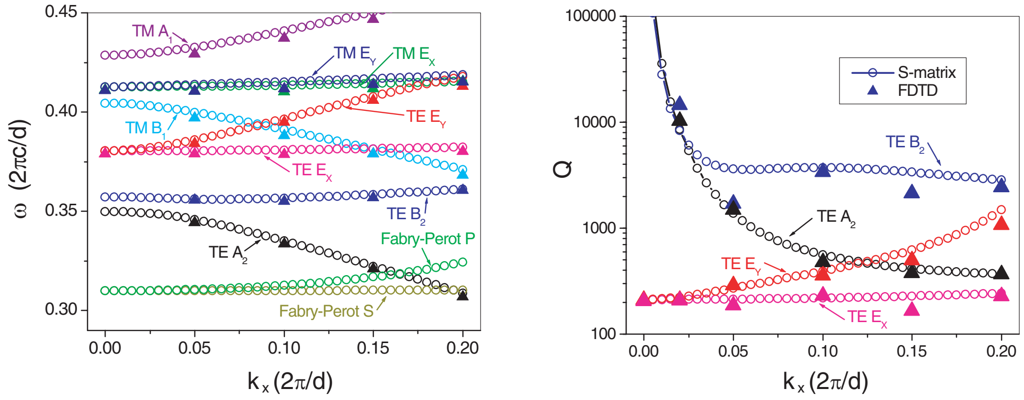

Fig. 4 The dispersion (left panel) and quality factor (right panel) of the lowest Fabry–Perot and quasiguided modes in PhCS with a square lattice of holes in GaAs slab (dielectric constant $\varepsilon = 12$, radius of holes $r = 0.2d$, d – period, thickness $h = 0.5d$.) Results of the *S*-matrix calculations [25] (open circles) are compared with the FDTD results for the same structure from [32] (solid triangles). Note a very good agreement of the calculated spectra at lower frequencies.

spectra of such structures are characterized by an additional sharp resonance feature due to the excitation of quasiguided modes of the corrugated waveguide. Strong coupling between these optical modes and the particle plasmon resonances of the nanowires results in the formation of a waveguide-plasmon polariton with a large Rabi splitting of nearly 250 meV. Scattering matrix theory gives an excellent agreement between all experimentally measured and theoretically modelled extinction spectra.

Acknowledgements This work was financially supported by the German Bundesminister für Bildung und Forschung (FKZ 13N8340/1), the Deutsche Forschungsgemeinschaft (Priority Program SP1113), and in part by the Russian Foundation for Basic Research, the Russian Ministry of Science, and the Russian Academy of Sciences. The authors are grateful to K. von Klitzing for continuous support and to T. Ishihara, S. Linden, E. A. Muljarov, N. C. Nielsen, and V. V. Popov for discussions.

References

[1] E. Yablonovitch, Phys. Rev. Lett. **58**, 2059 (1987).
[2] S. John, Phys. Rev. Lett. **58**, 2486 (1987).
[3] J. D. Joannopoulos, R. D. Meade, and J. N. Winn, Photonic Crystals (Princeton Univ. Press, Princeton, NJ, 1995).
[4] M. Nevière, E. Popov, R. Reinisch, and G. Vitrant, Electromagnetic resonances in nonlinear optics (Gordon and Breach, 2000).
[5] K. Sakoda, Optical properties of photonic crystals (Springer, 2001).
[6] R. W. Wood, Philos. Mag. **4**, 396 (1902).
[7] Lord Rayleigh, Philos. Mag. **14**, 60 (1907).
[8] E. L. Ivchenko, A. Nesvizhskii, and S. Jorda, Phys. Solid State **36**, 1156 (1994).
[9] V. P. Kochereshko, G. R. Pozina, E. L. Ivchenko, D. R. Yakovlev, A. Waag, W. Ossau, G. Landwehr, R. Hellmann, and E. O. Göbel, Superlatt. Microstruct. **15**, 471 (1994).
[10] M. Hübner, J. Kuhl, T. Stroucken, A. Knorr, S. W. Koch, R. Hey, and K. Ploog, Phys. Rev. Lett. **76**, 4199 (1996).
[11] L. Pilozzi, A. D'Andrea, and R. DelSole, Phys. Rev. B **54**, 10763 (1996).
[12] T. Fujita, Y. Sato, T. Kuitani, and T. Ishihara, Phys. Rev. B **57**, 12428 (1998).
[13] R. H. Ritchie, E. T. Arakawa, J. J. Cowan, and R. N. Hamm, Phys. Rev. Lett. **21**, 1530 (1968).
[14] S. C. Kitson, W. L. Barnes, and J. R. Sambles, Phys. Rev. Lett. **77**, 2670 (1996).
[15] S. I. Bozhevolnyi, J. Erland, K. Leosson, P. M. W. Skovgaard, and J. M. Hvam, Phys. Rev. Lett. **86**, 3008 (2001).

[16] W. L. Barnes, A. Dereux, and T. W. Ebbesen, Nature **424**, 824 (2003).
[17] T. W. Ebbesen, H. J. Lezec, H. F. Ghaemi, T. Thio, and P. A. Wolff, Nature **391**, 667 (1998).
[18] S. Linden, J. Kuhl, and H. Giessen, Phys. Rev. Lett. **86**, 4688 (2001).
[19] E. R. Brown and O. B. McMahon, Appl. Rev. Lett. **67**, 2138 (1995).
[20] E. Cubukcu, K. Aydin, E. Ozbay, S. Foteinopoulou, and C. M. Soukoulis, Nature **423**, 605 (2003).
[21] A. Christ, S. G. Tikhodeev, N. A. Gippius, J. Kuhl, and H. Giessen, Phys. Rev. Lett. **91**, 183901 (2003).
[22] A. Christ, T. Zentgraf, J. Kuhl, S. G. Tikhodeev, N. A. Gippius, and H. Giessen, Phys. Rev. B, to be published (2004).
[23] H. Raether, Surface Plasmons on Smoth and Rough Surfaces and on Gratings (Springer, Berlin, 1988).
[24] U. Kreibig and M. Vollmer, Optical Properties of Metal Clusters (Springer, Berlin, 1995).
[25] S. G. Tikhodeev, A. L. Yablonskii, E. A. Muljarov, N. A. Gippius, and T. Ishihara, Phys. Rev. B **66**, 045102 (2002).
[26] U. Fano, J. Opt. Soc. Am. **31**, 213 (1941).
[27] P. B. Johnson and R. W. Christy, Phys. Rev. B **6**, 4370 (1972).
[28] R. Parmentier et al., private communication.
[29] C. D. Ager and H. P. Hughes, Phys. Rev. B **44**, 13452 (1991).
[30] D. M. Whittaker and I. S. Culshaw, Phys. Rev. B **60**, 2610 (1999).
[31] N. A. Gippius, S. G. Tikhodeev, and T. Ishihara, arXiv:cond-mat/0403010 (2004).
[32] S. Fan and J. D. Joannopoulos, Phys. Rev. B **65**, 235112 (2002).